Field behaviour of driven Pre-stressed High-strength Concrete piles in sandy soils

ZX Yang[1], WB Guo[2], FS Zha[3], RJ Jardine[4], CJ Xu[5], YQ Cai[6]

Abstract

Driven piles are used widely both offshore and onshore. However, accurate axial capacity and load-displacement prediction is difficult at sand dominated sites and offshore practice is moving towards Cone Penetration Test (CPT) based design methods developed from instrumented pile research and database studies. However, onshore use of these methods remains limited; there is a paucity of high quality case-histories to assess their potential benefits clearly and application in layered profiles may be uncertain. This paper presents new tests on Pre-stressed Concrete (PHC) pipe-piles driven in sands for a major new Yangtze River bridge project in China, assessing the performance of the 'new CPT' and conventional capacity approaches, considering the influence of weak sub-layers on base resistance and noting the marked changes in shaft capacity that apply over time.

Keywords: PHC driven pile; cone penetration test; onshore; sand; capacity; layered profile; time effect and aging

Introduction

Large driven piles are often used to support long-span bridges, port facilities or offshore platforms and wind turbines. While steel pipe piles dominate offshore, Pre-stressed High-strength Concrete (PHC) piles are used widely in China for high-rise buildings, river

[1]Associate Professor, Research Centre of Coastal and Urban Geotechnical Engineering, Dept. of Civil Engineering, Zhejiang University, China, zxyang@zju.edu.cn
[2]PhD student, Dept. of Civil Engineering, Zhejiang University, China, guowb2008@zju.edu.cn
[3]Professor, School of Recourses and Environmental Engineering, Hefei University of Technology, China, zhafusheng@163.com
[4]Professor, Dept. of Civil and Environmental Engineering, Imperial College, UK, r.jardine@imperial.ac.uk
[5]Professor, School of Civil Engineering and Architecture, East China Jiaotong University, Nanchang, China; Dept. of Civil Engineering, Zhejiang University, China, xucj@ecjtu.edu.cn
[6]Professor, Research Centre of Coastal and Urban Geotechnical Engineering, Dept. of Civil Engineering, Zhejiang University, China, caiyq@zju.edu.cn

crossings, high-speed railways, ports and piers. PHC piles are normally pre-cast open-ended cylinders with outside diameters of 300-1000mm and 70-130mm wall thicknesses that are assembled on-site by welding circumferential steel connection plates. Installation usually involves driving or jacking; a vibration and pre-drilling has also been utilized.

Most international offshore projects apply API RP2GEO (2014) or the equivalent ISO design recommendations. While the API and ISO methods are employed internationally for some major bridge and harbor projects, local technical foundation specifications apply more frequently in onshore work and JGJ 94-2008 (CABR2008) is the most common design rule for large structures in China. Pile load tests are often called for as conventional design methods are known to be subject to relatively poor reliability and potential bias (Briaud and Tucker 1988). However, such tests are usually unfeasible in offshore projects. Rigorous database studies show that measured driven pile test capacities (Q_m) can vary very significantly from those expected from calculation (Q_c), especially for piles driven in sands. For example, Chow (1997), Kolk et al. (2005), Jardine et al. (2005) and Schneider et al. (2008) all found that compressive capacity predictions made with the industry-standard 'Main text' API (2014) approach are subject to overall CoVs in Q_c/Q_m of 0.60 to 0.88. The latter two studies explored the degrees of bias found with respect to the pile Diameter D, slenderness L/D, and the average relative densities (D_r) applying over the shafts and tips. They showed that the API 'Main Text' method gives least scatter and Q_c/Q_m closest to unity in cases with $40 \le L/D \le 65$, $35\% \le Dr \le 65\%$ and $0.4m \le D \le 0.8m$. When all other factors are held constant, the shaft resistance expression tends to become non-conservative with: higher L/D ratios, looser sands and in tension. Base resistance can also be over-predicted when $D \ge 0.8m$. The opposite trend applies in denser sands in cases that fall below the above L/D and Diameter lower bounds. Williams et al (1997), Jardine et al (2005) and Overy (2007) report case histories where the Main Text approach led to Q_c/Q_m values ranging from 0.4 to 2.9. Jardine and Chow (2007) discussed how such discrepancies could be reconciled with the low incidence of reported offshore foundation failures, concluding that unanticipated beneficial effects of time on shaft resistance contributed to the perception of satisfactory performance, along with the sand and pile conditions typically encountered offshore. The present lack of offshore pile monitoring that could detect the axial movements (of perhaps ≈D/100) at which shaft failure can develop is also relevant.

Instrumented field and model instrumented piles (Lehane et al. 1993, Chow 1997, Gavin and Lehane 2003, Yang et al. 2010, Jardine et al. 2013a and 2013b, Yang et al. 2014) offer new insights into the fundamental behavior of driven piles and the basis for simple design methods that capture more faithfully the stress conditions developed by driving, the fundamental shaft failure mechanisms and the key factors that govern base resistance. API RP2GEO (2014) recognizes its Main Text approach's limitations and the potential of four alternative CPT-based methods set out in its commentary from: Fugro-05 (Kolk et al. 2005), Imperial College London (ICP-05, Jardine et al 2005, albeit in a 'simplified form'), Norwegian Geotechnical Institute (NGI-05, Clausen et al 2005), and University of Western Australia (UWA-05, Lehane et al 2005). Crucial to all is recognition that end bearing and shaft resistances are more sensitive than expected to local variations in sand state, which they capture through CPT profiling. The new methods also: (i) address explicitly the previously unrecognized dependence of the radial stresses developed on the pile shaft at any given level on the relative depth *h* of the pile tip and (ii) give closer attention to the effect of tip geometry on base capacity. A comprehensive assessment by Schneider et al. (2008) showed the 'CPT' approaches giving lower Q_c/Q_m CoVs than the API Main Text treatment. The UWA-05 and ICP-05 methods offered the best overall reliability, with mean Q_c/Q_m close to unity and CoV values below 30%. While API RP2GEO (2014) remarks on the CPT methods' limited historical use, the ICP-05 has now developed a significant track-record: see for example Williams et al (1997), Overy (2007) or Merritt et al (2012).

The international pile test databases include surprisingly few high quality tests to failure on large pipe-piles driven in sand at sites with full CPT profiles. For example, the well-known French LCPC/IFSTTAR dataset (Bustamante and Gianeselli 1982, Frank and Burlon 2012) contains no such entry. The most comprehensive sets appear to be those assembled by Jardine et al (2005) and Schneider et al (2008) which include over 100 different piles driven in silica sand and tested to failure. However, only 11 piles tested at just three sites were open-ended, had D≥600mm and full CPT profiles. No concrete pipe pile and only two Asian test sites were included. Further tests are required to (i) augment this sparse dataset, (ii) address uncertainty over end bearing in layered strata, (iii) assess whether the CPT methods apply to concrete piles and silty sands and (iv) give further insight into the effects of pile age on capacity as reported by Jardine et al (2006) and Gavin et al (2013). This paper contributes as part of an on-going Zhejiang University/Imperial College London database project four new good quality static loading tests conducted to failure at three Chinese sites with full CPT profiles.

The test piles were driven to either side of the Second Wuhu Bridge crossing of the Yangtze

River in Anhui Province, China, 100 km SE of Hefei. The bridge will be ≈14km long and its central cable-stayed steel box girder bridge spans 1,622m. Driven PHC piles are used to support the many approach piers driven on both sides of the river into Quaternary, mainly sand, alluvium transported from weathered rock colluvium eroded from upstream locations. We focus first on piles PHC-1 to 3 that have sand-dominated profiles and were tested statically 13 to 15 days after driving. Attention is then turned to an 'untypical' pile PHC-4 that was (i) driven to a final penetration underlain at modest depth by a clay layer and (ii) tested at a relatively young 'age', 5 days after driving. We acknowledge that adding strain gages or conducting tension tests would have helped separate the shaft and base resistances. However, even when this is possible, great care is required to address 'gage-drift' after driving as well as temperature and radial stress cross-sensitivity effects. A carefully designed study of aging trends would also have been helpful. Nevertheless, the tests conducted provide clear outcomes concerning the axial capacity assessment, pile-soil stiffness, pile age and the importance of accounting for weak substrata when predicting base resistance.

Pile details and test ground conditions

Piles PHC-1, PHC-3 and PHC-4 outer diameters D=600mm while that for PHC-2 was 800mm. All had a uniform wall thickness t=130mm, were formed from grade C80 concrete (reinforced to give section moduli, EA of 7,300 and 10,400 MN respectively) and were driven by a 10.3T drop-hammer employing a drop height of 1.8 m. No pile toe modification was used to aid driving. Table 1 summarizes the pile make-up, dimensions and driving details, while Fig. 1 shows the bridge and test pile layout at sites K34 (PHC-1, south-east of the River), K27 (PHC-2 seven km to the north-west) and K24+500 (PHC-3 and 4, 2.5 km north-west from

K27) where subsurface conditions comprise mainly silty and fine sands, with thin agricultural soil over muddy silty clay in the top 0 to 4m. The ground water tables were all relatively close to ground level. Site K24+500 also presented a thin layer of silty clay between ≈35 and 36m depth. Cone penetration tests (CPT) were performed at each test site, and their cone resistance q_c and are compared directly in Fig 2a). Site K24+500 has the 'loosest' profile and K34 the 'densest'. Figure 2b) presents relative density D_r profiles derived from CPT q_c profiles by the Jamiolkowski et al. (2003) expressions; broadly similar profiles are obtained in this case if one adopts the earlier Baldi et al (1986) expressions. We interpret the thin layers appearing to show D_r≤20% as comprising silts or clays. Site investigations indicated saturated unit weights of 19-20kN/m^3 for the sands and ≈16 kN/m^3 for the clays. Figure 3 shows the spread of soil grading curves. The mean D_{50} values of the silty and fine sands are 0.15 mm and 0.18 mm, respectively, while the <0.075mm fines fraction is 23-31% for the silty sand and 8-10% for the fine sand. Direct shear tests on the silty sand and fine sands show $26^o \leq \phi' \leq 29^o$, assuming zero c'. No site-specific interface tests were available. However, ring-shear experiments reported by Barmpopoulos et al (2009) involving a wide range of clean silica sands and concrete indicate large-displacement interface shear resistance angles that depend on the pile roughness-to-soil D_{50} ratio and indicate for these piles a critical state δ'_{cv}= 29^o that coincidentally matches the value proposed for steel piles in Fugro-05 and UWA-05.

Static load test

Two phases of multiple tests were conducted on the bridge's PHC piles. We consider only the four PHC pipe-piles driven in dominantly sandy soils for which nearby high quality CPT tests are available. As listed in Table 1, PHC-1, 2 and 4 were installed and tested in Phase I while PHC-3 was added in Phase II after PHC-4 gave disappointing results. Table 1, Fig. 4a) and Fig. 4b) summarizes how driving progressed with penetration depth. No measurements were made of the sand plug. However, the UWA-05 methodology described later predicts final Incremental Filling Ratios (IFRs) between 74 and 82% for all piles.

The load tests employed the arrangements shown in Fig. 5. It is likely that any untested piles' shaft resistances would have grown considerably in the weeks and months that followed driving; see Jardine et al (2006). The reported static tests on PHC-1 to 3 followed 13 to 15 days after driving, with the automated hydraulic loading system reacting against large concrete kentledge masses. The loads were measured through the hydraulic oil pressure system and the displacements monitored by four digital dial gauges fixed to reference beams supported by steel poles driven at some distances away from the loading platform. The first load increment was 1200 *k*N, while the subsequent increments were each 600 *k*N. Load steps were applied each hour until abrupt increases were seen in pile head displacement. The complete load-displacement curves for piles PHC-1, PHC-2 and PHC-3, are given in Fig. 6, which identifies the overall resistance developed after displacements s=0.1D. Tables 1 to 2 summarize the pile configurations and load test outcomes. The larger diameter of PHC-2 contributed to it having the largest capacity. PHC-3 was driven to the greatest depth (in Phase II) because PHC-4 had developed (in Phase I) a far lower capacity than PHC-1 or 2, whose site conditions and pile lengths had been thought comparable. Following Fleming et al (2009), indicative 'shaft-yield' loads are listed at which settlements reached D/100 and may correspond approximately to the stages where peak shaft resistances were mobilized.

We discuss later how strata, penetration depth and age may have affected the anomalous test on PHC-4.

Piles PHC-1 to 3 exhibited both broadly similar load-displacement responses, as shown in Fig. 6). Table 3 lists initial secant pile head stiffness initial values $k_{Ref} = \Delta Q/\Delta s$ determined for each pile from the first 1200 kN load increment applied (Q_{Ref}), while Fig. 7a) demonstrates their subsequently steeply non-linear stiffness trends in normalized k/k_{Ref} - Q/Q_{Ref} plots. Also listed in Table 3 are initial sand shear stiffness G_{Ref} values found for the mid-pile depth position (under Q_{Ref}) by applying the Randolph (1977) analysis for compressible piles in elastic soils. While stiffness was assumed to be proportional to depth, checks made assuming uniform conditions show only marginally (≤10%) lower G values. Overall, PHC-1 shows the highest G_{Ref} and k_{Ref} values, reflecting perhaps its generally 'denser' shaft CPT profile. However, this pile also shows the steepest decay of normalized k with load in Fig. 7a). The same trend is clear in Fig. 7b), which reveals how secant G/G_{Ref} ratios (found elastic analysis of each load step) degraded with Q/Q_{Ref}.

Randolph (1977) also derived from his elastic analysis expressions for the shaft-to-base load split and Table 3 applies these to the listed nominal 'shaft yield' points, indicating that only 1 to 6% of the total loads mobilized at s=D/100 went to the bases. These estimates led to the nominal shaft capacity Q_s estimates listed in Table 3. Assuming that shaft failure is ductile, as found in highly instrumented tests by Lehane et al (1993) and Chow (1997), allowed nominal base capacities Q_b to be assessed for the s=D/10 stages by deducting the indicative Q_s values from the total measured loads. We acknowledge that the base-to-shaft split is highly approximate: elastic analyses cannot be expected to be accurate for large piles in non-linear soils: see Jardine et al (1986). The base and shaft capacities could have been separated more securely if strain gages had been installed, or tension tests conducted.

Capacity prediction

The PHC pile parameters listed in Tables 1 and 4 all fall within the ranges 36<L/D<66, 33%<mean D_r<65% and 0.6m<D<0.8m. As mentioned earlier, independent database studies indicate that the two CPT methods and API Main text approach should give broadly satisfactory medium-term total capacity predictions within these ranges. The API scheme assumes that local shaft and base resistances grow in proportion with the free field vertical effective stress (σ'_{vo}) and are relatively insensitive to changes in sand state with depth. It does not recognize any relative pile tip depth dependency of shaft resistance but specifies upper limits to the unit shaft and base resistances. The ICP-05 and UWA-05 methods consider other factors that influence the radial stresses acting on the pile shaft and consequently the capacity of the pile, including the local q_c values, the relative height (h) of any point on the shaft above the tip, the pile end conditions and the free-field vertical effective stress.

None of the methods includes an explicit time allowance. While age is known to affect shaft capacity strongly, the early rates of capacity growth after driving are not fully clear. The average age after driving within the database against which the ICP was tested was 25 days. However, the ICP capacity was available at an earlier stage (after ≈10 days) in field ageing tests by Jardine et al (2006) and slightly faster shaft capacity growth was reported over the first 12 days after driving by Gavin et al (2013).

The static axial bearing capacity Q_c of a pile under compression loading at a displacement of

0.1D is the sum of the shaft capacity Q_s and base capacity Q_b:

$$Q_c=Q_s+Q_b=\pi D\int\tau_f dz+q_{b,0.1}A_b \qquad \text{Eq. (1)}$$

where *D* is the pile diameter; τ_f is the local ultimate shaft friction; z is depth; $q_{b,0.1}$ is the end bearing available after displacement by D/10 and A_b is the base area. Different $q_{b,0.1}$ expressions apply in ICP-05 and UWA-05. For ICP-05, $q_{b,0.1}$ is expressed as,

$$\begin{cases}\text{unplugged}: q_{b,0.1}=q_{c,avg}[1-(D_i/D_o)^2]\\ \text{plugged}: q_{b,0.1}=q_{c,avg}\max[0.14-0.25\log D_o, 0.15, 1-(D_i/D_o)^2]\end{cases} \qquad \text{Eq. (2)}$$

in which D_o and D_i are the outer and inner diameters and $q_{c,avg}$ is averaged (under routine conditions) over an interval ±1.5D above and below the pile tip. However, Jardine et al (2005) note that *"the selection of appropriate q_c values should account for the form of the CPT traces. Because the postulated annular end bearing mechanism can develop over a relatively short depth range of perhaps three pile wall thicknesses, the design value should reflect the weakest sufficiently thick sub-layer within the soil unit in which the pile tip might credibly be terminated. Equally, consideration should be given to the possibility of a more critical fully plugged failure mode developing if a generally weaker layer exists within 8 pile diameters of the expected final tip depth."* More recently, the ICP-05 authors have proposed that while shaft resistance design assessments can be based on best estimate (average) q_c profiles, a lower bound profile should be adopted for base capacity.

With UWA-05, $q_{b,0.1}$ is calculated by,

$$q_{b,0.1}=q_{c,avg}[0.6-0.45(D_i/D_o)^2\text{IFR}] \qquad \text{Eq. (3)}$$

where IFR is the incremental filling ratio, and $q_{c,avg}$ is evaluated by the Dutch technique, which considers the q_c profile over a greater depth range that the ICP.

The local ultimate shaft friction τ_f in Eq. (1) is calculated in ICP-05 as,

$$\tau_f=[0.029q_c(\sigma'_{vo}/p_A)^{0.13}[\max(h/R^*,8)]^{-0.38}+\Delta\sigma'_{rd}]\tan\delta_f \qquad \text{Eq. (4)}$$

in which σ'_{vo} is free-field vertical effective stress; p_A is the atmospheric pressure; R^* is the equivalent pile radius; *h* is the relative height above the tip and δ_f is found from interface ring shear tests or from correlations with mean grain size (D_{50}); $\Delta\sigma'_{rd}$ the dilatant increase in local radial stress during pile loading can be obtained by:

$$\Delta\sigma'_{rd}=2G\Delta r/R \qquad \text{Eq. (5)}$$

where *G* is the operational shear modulus (estimated from correlations with CPT q_c and σ'_{vo}) and Δr is the radial displacement related to pile shaft roughness, which is taken as 0.02mm for industrial (lightly rusted) steel piles. With open piles an equivalent radius R^* is used to replace R is Eq. 4, calculated from the pile's outer and inner radii (R_o and R_i) as $R^*=(R_o^2-R_i^2)^{1/2}$.

UWA-05 employs a variant of Eq. (2) to calculate the local ultimate shaft friction,

$$\tau_f=[0.03q_cA_{rs,eff}^{0.3}[\max(h/2R,2)]^{-0.5}+\Delta\sigma'_{rd}]\tan\delta_f \qquad \text{Eq. (6)}$$

in which $A_{rs,eff}$ =1-IFR$(Ri/R)^2$ is the effective area ratio. The UWA approach applies Eq. (5) to estimate $\Delta\sigma'_{rd}$ but its different G-q_c correlation function gives marginally different results.

It is necessary when applying the UWA method to specify the full IFR profile. The latter can be measured on site and employed in hind-casts, but cannot be known in advance. UWA-05 offers Eq. 7 to estimate IFR in design predictions or hindcast analyses, where ΔL_p is the change in plug length and Δz is the change in penetration per blow. Lehane et al (2005) propose that IFR should be set to unity and $\Delta\sigma'_{rd}$ to zero for offshore applications.

$$\text{IFR}=\Delta L_p/\Delta z=\min[1,(D_i(m)/1.5)^{0.2}] \qquad \text{Eq. (7)}$$

As noted earlier, $\delta_f=\delta'_{cv}$ was taken as 29° for the ICP and UWA calculations (after Barmpopoulos et al. 2009); Δr was also taken as 0.02mm (as with steel piles). Noting that the three site profiles include some minor clay layers at shallow depth and that there is a thin clay layer in K24+500, Lehane et al's (2005) approximate estimate for local shaft resistances $\tau_f \approx q_c/35$ was applied in any thin clay strata present over the shaft length, where q_c was the local cone resistance, with the that clay layers contributing <1% of shaft capacity. Table 4 gives the tip q_c values, the average $q_{c,avg}$ derived by the alternate procedures and the relative densities adopted in assessing the capacities of these four piles. Table 5 summarizes the calculations made for PHC-1 to PHC-3 using the API, full-ICP and UWA (both full and offshore) methods. Noting the difficulties of separating the measured shaft and base components, we consider the overall total Q_c/Q_m ratios. The average ratio for ICP-05 is 1.09, while means of 0.91 and 0.79 apply to 'full' and 'offshore' UWA assessments; the API Main Text approach gives a mean Q_c/Q_m= 0.80.

Potential explanations for the 'anomalous' Test PHC-4

As noted earlier, Pile PHC-4 developed a far lower capacity than PHC-1 to 3. Fig. 8a) compares its load-displacement behavior with PHC-3, which was installed at the same location, but to a different tip penetration (see Fig. 2), while Fig. 8b) shows the corresponding stiffness degradation trends. Factors that may have led to this outcome include:

- This test being staged 5 days after installation, while the others were conducted after 13 to 15 days
- A thin clay band located 4.3 to 6.3D beneath the pile tip (see Fig 2)
- Local variations in ground conditions between the CPT and pile locations, which were set 3.2m apart.

The load displacement curves for the two K24+500 test piles PHC-3 and PHC-4 are compared in Fig. 8, showing that the 'early-age' PHC-4 test mobilized its shaft resistance after smaller displacements. The axial load was just 1.2MN at 6mm and the Randolph (1977) analysis outlined earlier indicates that the shaft carried almost all (97%, see Table 3) of this applied load. The later stages of both tests show parallel load-displacement curves with base capacity building at ≈15kN/mm, without any clear peak or reduction in gradient; Table 3 summarizes the indicative shaft-to-base load split determined as outlined earlier.

Time effects

We can apply the shaft capacity time-age curves developed by Jardine et al (2006) to gage what effect age after driving might have had on first-time shaft capacity. As noted by Tavenas and Audy (1972) and Rimoy (2013) overall static compression capacities grow at slower rates, because their base components remain relatively unaffected by time. Relatively little data exists to define the early age shaft set-up, but the trends defined by Jardine et al (2006) imply that the 5 day capacity should be 15% lower that the ICP capacity. Recent tests by Gavin et al (2013) indicate slightly faster earlier growth rates. While pile age corrections reduce the PHC-4 shaft capacity mismatch, they cannot explain all of the observed discrepancy.

Table 6 offers a comparison between the interpreted PHC-4 shaft capacity after applying a 15% correction for time effects and those derived by the ICP and UWA methods, as applied with their 'default' q_c averaging techniques. The corrected interpreted shaft resistance still falls 28% below the default ICP estimate, while the full UWA approach leads to a slightly closer match, and the API main text method over-predicts the capacity by 121%.

Influence of the weak substratum

We consider next the potential effect on PHC-4 of the silty clay layer, which showed q_c minima around 3.6MPa (Fig. 2) between 35.6 and 36.8m depth in a nearby sounding, while PHC-4's tip penetrated to 33.0m. First we note that subtracting the nominal 1.2MN shaft capacity interpreted above from the 2MN load developed after a settlement of D/10 implies a base capacity of just 0.8MN. Table 7 compares this base resistance with that obtained from the ICP and UWA procedures applying both the 'default' procedures and other approaches. It can be seen that simply averaging the q_c traces positioned 1.5D_o above and below the tip (where 8< q_c<14 MPa) leads to a considerable ICP over-estimate for the base capacity. Recognizing the underlying soft layer and adopting a 3.6MPa lower bound (as presently recommended by the ICP authors) leads to a far closer estimate. As summarized in Table 7, the 'Dutch' averaging method recommended in UWA-05 improves this method's match but still exceeds the interpreted field value by 44%. However, a closer match would be obtained in this case if the Dutch method was modified by extending its 4D lower limit. Any extension beyond 4.3D would be sufficient to capture the potential effect on PHC-4 of the first thin band of softer clay. The main text API method only slightly overestimates the interpreted base capacity by 13%.

Xu (2006) investigated closed-ended conical piles penetrating into layered strata through both numerical analysis and centrifuge testing. She considered a three-layer system comprising a weak clay seam underlain and overlain by strong sandy layers, which she termed 'strong/weak/strong'. She found reductions in base capacity and stiffness caused by a weak clay seam below the tip that depended on weak layer's thickness T_w and the depth to its upper surface H. Applying her plots to the PHC-4 pile geometry with $T_w/D=2$ and $H/D=4.3$ suggests a reduction factor ≈0.73 in the end bearing capacity due to the underlying weak layer that would bring the ICP or UWA predictions into better agreement with the interpreted field data, as outlined in Table 7. Yu and Yang (2012) proposed a base capacity method, termed the HKU method, in which the governing influence zone depends on embedded conditions, sand compressibility, and q_c profile variations. They consider that base capacity to be more influenced by the soil beneath than above the pile tip. As shown in Table 7, the HKU method gives the closest estimate for the base capacity interpreted above for PHC-4. The presence of the clay layer may have also downgraded the shaft resistance. Given that the base capacity profile 'sensed' the weak layer, it is also likely to have reduced the radial stresses built-up over the shaft just behind the tip, which often contributes a major part of the pile's capacity. Overall, early testing and the underlying weak clay layer appear to be plausible factors in explaining PHC-4's low shaft and base capacities.

Stratum variability

Variability in the local stratigraphy is a further factor that may have contributed to the lower-than-expected capacity of PHC-4. The silty sand and silty clay layers could vary over relatively short distances, as shown by the two logs in Fig. 9 from two boreholes positioned 40m apart to either side of PHC-4 (K24+500) at K24+482 and K24+522 respectively. The PHC-4 q_c profile was taken from a CPT test conducted within 3.2 meters of the pile, but reductions in the depth to the clay layer's upper surface, or variations in the depth of 'low-spots' in the silty sand profiles could have affected on the base capacity assessment made by any of the procedures outlined above. It appears prudent under such circumstances to adopt lowest credible q_c profiles to be safe when assessing design base capacities.

Conclusions

Currently published databases suffer from a paucity of tests to failure on industrial sized pile-piles driven in sands at sites with full CPT profiles. The scarcity of field data appears to be impeding the adoption of design methods that offer fundamentally better physical models and greater reliability. This paper presents and interprets a new set of static tests on pipe piles driven through mainly sandy strata at three sites located several km apart; good quality local CPT soundings are available for each location. Deploying strain gages, conducting tension tests and investigating time effects would have aided test interpretation. However, the information gathered, combined with reference to earlier published studies, allows six main conclusions to be drawn:

1) The API Main text, ICP-05 and UWA-05 all offered fair predictions for the total axial compression capacities of Piles PHC-1 to PHC-3, as measured 13 to 15 days after driving. The API main text method predictions fell on average ≈20% below the measurements, which the ICP over-estimated on average by ≈9%. The 'full' UWA underestimated overall capacity by ≈9% and the 'simplified offshore' variant by ≈21%. The 'simplified' UWA or ICP variants appear unnecessarily conservative for piles such as those driven for the Yangtze bridge.

2) The relatively modest predictive errors fall well within the ranges established by broader database studies which show CoVs in Q_c/Q_m of ≈0.25 for the full ICP and UWA approaches and ≈0.7 for the API Main Text method. The same studies show that the latter's higher CoV arises principally from cases that fall outside the 40≤L/D≤65, 35%≤Dr≤65% and 0.4m≤D≤0.8m ranges that encompassed the Yangtze Bridge tests.

3) While the 'full' ICP and UWA CPT based approaches offer more reliable medium-term shaft capacity estimates over a wider range of conditions, their shaft capacity predictions should become progressively more conservative over time due to beneficial ageing processes.

4) The pile-soil axial load response was shown to be highly non-linear. Initial reference stiffness values and stiffness degradation curves have been interpreted that should be helpful to other applications.

5) A fourth pile, PHC-4, which was tested after just five days, gave an axial compressive capacity well below that expected by routine application of any of the three considered design methods. Time effects are likely to have contributed to the lower-than-expected shaft capacity interpreted in an approximate manner from the load-displacement curves. Early age testing is clearly undesirable.

6) A weak clayey substratum is considered to be the primary cause of the unexpectedly low base capacity of PHC-4. Approaches that consider explicitly weak layers lead to closer agreement with the field measurements. It is recommended that base capacity design assessments should rely on prudent 'lower bound' CPT q_c trends.

Acknowledgements

The research described was funded by the Natural Science Foundation of China (Grant Nos. 51178421, 51322809), the Chinese Ministry of Education Distinguished Overseas Professorship Programme, the National Key Basic Research Program of China (No.

SQ2015CB070563), Zhejiang University K.P. Chao's High Technology Development Foundation and the Fundamental Research Fund for Central Universities (No. 2014XZZX003-15). Their support is gratefully acknowledged. The third author also acknowledges his support from Natural Science Foundation of China (Grant Nos. 41172273 and 41372281).

Reference

American Petroleum Institute (API). (2014). ANSI/API recommended practice 2GEO, 1st Ed., RP2GEO, Washington, DC.

Barmpopoulos, I. H., Ho, T. Y. K., Jardine, R. J., and Anh-Minh, N. (2009). The large displacement shear characteristics of granular media against concrete and steel interfaces. Proc. Research Symposium on the Characterization and Behaviour of Interfaces (CBI). Atlanta, Frost, J.D. Editor, IOS Press, Amsterdam, 17-24.

Baldi, G., Bellotti, R., Ghionna, V., Jamiolkowski, M. and Pasqualini, E. (1986). Interpretation of CPT's and CPTU's, 2nd Part: Drained Penetration in Sands, Fourth Int. Geotechnical Seminar Field Instrumentation and In Situ Measurements, Nanyang Technological Institute, Singapore, November 1986, 143-156.

Bustamante, M., and Gianeselli, L. (1982). Pile bearing capacity prediction by means of static penetrometer CPT. Proc. 2nd European Symp. On Penetration Test., Balkema, Rotterdam, 493-500.

China Academy of Building Research (CABR). (2008). Technical code for building pile foundations. JGJ 94-2008, China Construction Industry Press, Beijing (in Chinese).

Clausen, C. J. F., Aas, P. M., and Karlsrud, K. (2005). Bearing capacity of driven piles in sand, the NGI approach. Proc., Int. Symp. On Frontiers in Offshore Geotechnics, Taylor & Francis, London, 677–681.

Chow, F.C. (1997). Investigations into displacement pile behaviour for offshore foundations. PhD thesis, University of London (Imperial College), UK.

Dai, Z. G., and Fang, X. (2005). A preliminary investigation into the soft soils in the river region of Wuhu. Geotechnical Engineering World, 8(1), 35-38 (in Chinese).

Frank, R., and Burlon, S. (2012). Personal communication.

Fleming, K., Weltman, A., Randolph, M, and Elson, K. (2009). Piling Engineering, 3rd Edition, Taylor & Francis, London and New York.

Gavin, K. G., Igoe, D. J. P., and Kirwan, L. (2013). The effect of ageing on the axial capacity of piles in sand. Proceedings of the ICE-Geotechnical Engineering, 166(2), 122-130.

Gavin, K. G., and Lehane, B. M. (2003). The shaft capacity of pipe piles in sand. Can. Geotech. J., 40(1), 36–45.

Jamiolkowski, M.B., Lo Presti, D.F.C., and Manassero, M. (2003). Evaluation of relative density and shear strength of sands from cone penetration test. Soil behaviour and soft ground construction, Geotechnical Special Publication, No. 119, ASCE, Reston, Va., 201-238.

Jardine, R. J., Chow, F. C., and Overy, R. (2005). ICP design methods for driven piles in sands and clays, Thomas Telford, London.

Jardine, R. J., Potts, D. M., Fourie, A. B., and Burland, J. B. (1986). Studies of the influence of non-linear stress–strain characteristics in soil–structure interaction. Géotechnique, 36(3), 377-396.

Jardine, R. J., Standing, J. R., and Chow, F. C. (2006). Some observations of the effects of time on the capacity of piles driven in sand. Géotechnique, 56(4), 227–244.

Jardine, R. J., and Chow, F. C. (2007). Some developments in the design of offshore piles. Proc., 6th Int. Conf. on Offshore Site Investigations and Geotechnics, Society for Underwater Technology, London.

Jardine, R. J., Zhu, B. T., Foray, P., and Yang, Z. X. (2013a). Measurement of stresses around closed-ended displacement piles in sand. Géotechnique, 63(1), 1–17.

Jardine, R. J., Zhu, B. T., Foray, P., and Yang, Z. X. (2013b). Interpretation of stress measurements around closed-ended displacement piles in sand. Géotechnique, 63(8), 613–627.

Kolk, H. J., Baaijens, A. E., and Sender, M. (2005). Design criteria for pipe piles in silica sands. Proc., Int. Symp. on Frontiers in Offshore Geotechnics, Taylor & Francis, London, 711–716.

Lehane, B. M., Jardine, R. J., Bond, A. J. & Frank, R. (1993). Mechanisms of shaft friction in sand from instrumented pile tests. J. Geotech. Engng Div. ASCE 119, No. 1, 19–35.

Lehane, B. M., Schneider, J. A., and Xu, X. (2005). A review of design methods for offshore driven piles in siliceous sand.UWA Rep. No. GEO 05358, The University of Western Australia, Perth, Australia.

Merritt, A., Schroeder, F., Jardine, R.J., Stuyts, B., Cathie, D. and Cleverly, W. (2012). Development of pile design methodology for an offshore wind farm in the North Sea. In: Proc. 7th Offshore Site Investigation and Geotechnics: Integrated Geotechnologies-Present and Future. London: SUT.

Overy, R. (2007). The use of ICP design methods for the foundations of nine platforms installed in the U.K. North Sea. Proc., 6th Int. Conf. on Offshore Site Investigations and Geotechnics, Society for Underwater Technology, London.

Randolph, M. F. (1977). A theoretical study of the performance of piles, PhD dissertation, University of Cambridge.

Rimoy, S. P. (2013). Ageing and axial cyclic loading studies of displacement piles in sands, PhD dissertation, Imperial College, London, UK.

Rimoy, S., Jardine, R.J and Standing, J.R. (2013). Displacement response to axial cycling of piles driven in sand. Geotechnical Engineering, 116 (2): 131-146.

Schneider, J.A., Xu, X., and Lehane, B. M. (2008). Database assessment of CPT-based design methods for axial capacity of driven piles in siliceous sands, Journal of Geotechnical and Geoenvironmental Engineering, ASCE, 134(9), 1227-1244.

Tavenas, F., and Audy, R. (1972). Limitations of the driving formulas for predicting the bearing capacities of piles in sand. Canadian Geotechnical Journal, 9(1), 47-62.

Williams, R.E., Chow, F.C. and Jardine, R.J. (1997). Proc. Int. Conf. on Foundation Failures. IES, NTU, NUS and Inst. Structural Engineers, Singapore, 363-378.

Xu, X. (2006). Investigation of the end bearing performance of displacement piles in sand. The University of Western A2006ustralia, PhD dissertation, Perth, Australia.

Xu, X., Schneider, J.A., and Lehane, B.M. (2008). Cone penetration test (CPT) methods for end bearing assessment of open- and closed-ended driven piles in siliceous sand. Canadian Geotechnical Journal, 45, 1130-1141.

Yu, F., and Yang, J. (2012). Base capacity of open-ended steel pipe piles in sand. Journal of

Geotechnical and Geoenvironmental Engineering, ASCE, 138(9), 1116-1128.

Yang, Z. X., Jardine, R. J., Zhu, B. T., Foray, P., and Tsuha, C.H.C. (2010). Sand grain crushing and interface shearing during displacement pile installation in sand. Géotechnique, 60(6), 469-482.

Yang, Z.X., Jardine, R.J., Zhu, B.T., Rimoy, S. (2014). The stresses developed round displacement piles penetrating in sand, Journal of Geotechnical and Geoenvironmental Engineering, ASCE, Doi: 10.1061/(ASCE)GT.1943-5606.0001022, 04013027.

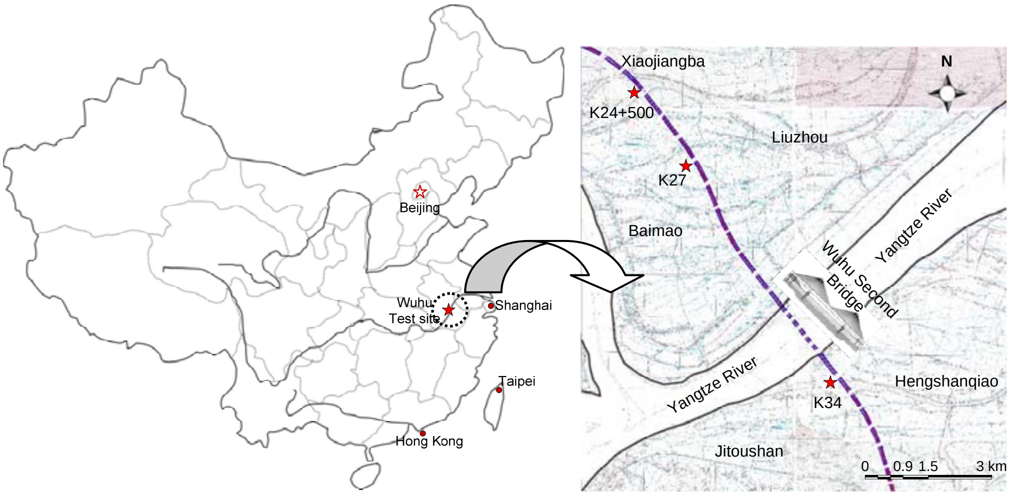
Beijing
Wuhu
Test site
Shanghai
Taipei
Hong Kong
Xiaojiangba
K24+500
N
Liuzhou
K27
Baimao
Yangtze River
Wuhu Second Bridge
Yangtze River
K34
Hengshanqiao
Jitoushan
0 0.9 1.5 3 km

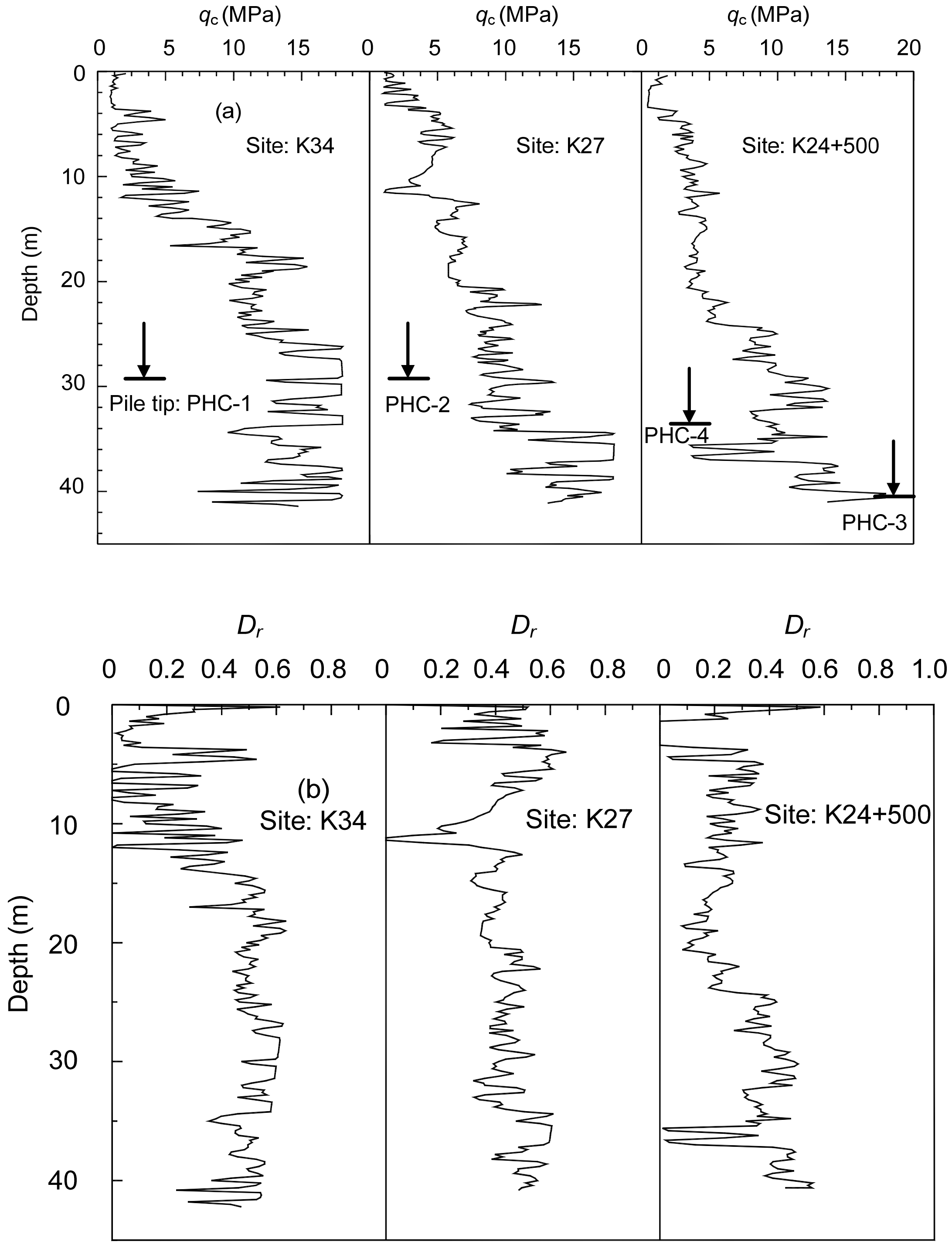

q_c (MPa)
q_c (MPa)
q_c (MPa)
0 5 10 15 0 5 10 15 0 5 10 15 20
(a)
Site: K34
Site: K27
Site: K24+500
Depth (m)
0 10 20 30 40
Pile tip: PHC-1
PHC-2
PHC-4
PHC-3
D_r
D_r
D_r
0 0.2 0.4 0.6 0.8 0 0.2 0.4 0.6 0.8 0 0.2 0.4 0.6 0.8 1.0
(b)
Site: K34
Site: K27
Site: K24+500
Depth (m)
0 10 20 30 40

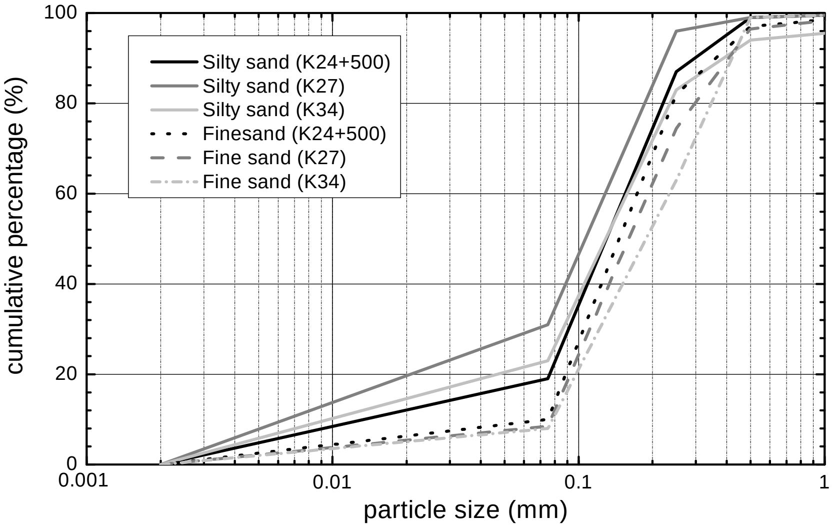

Silty sand (K24+500)
Silty sand (K27)
Silty sand (K34)
Finesand (K24+500)
Fine sand (K27)
Fine sand (K34)
cumulative percentage (%)
particle size (mm)
0
20
40
60
80
100
0.001
0.01
0.1
1

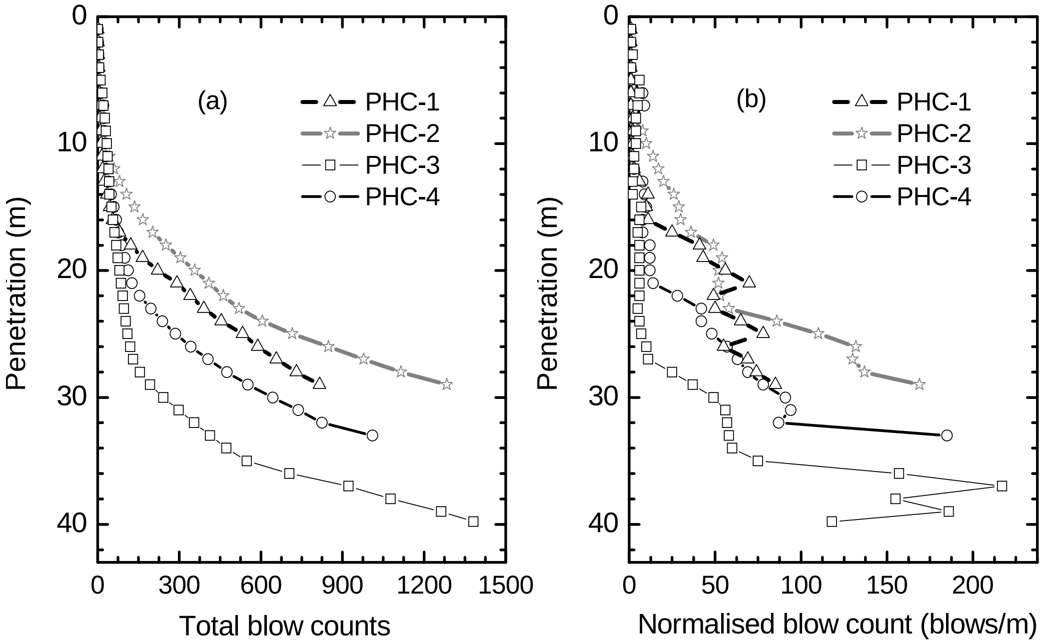

(a)
PHC-1
PHC-2
PHC-3
PHC-4
Penetration (m)
Total blow counts
0
10
20
30
40
0
300
600
900
1200
1500
(b)
Normalised blow count (blows/m)
50
100
150
200

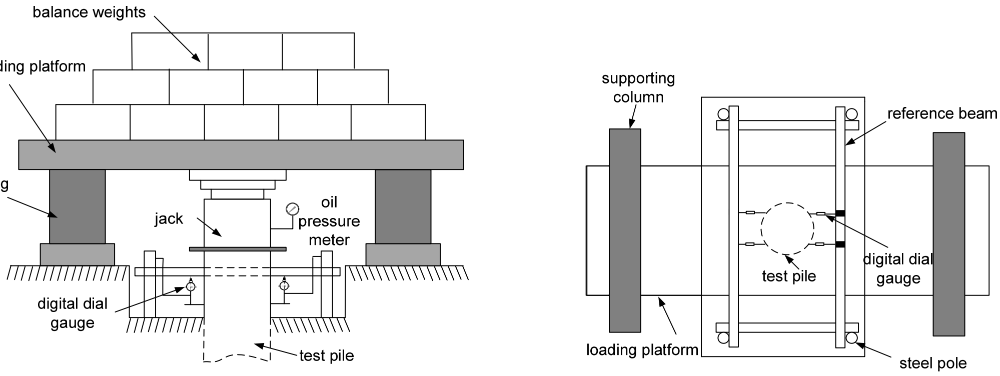
balance weights
loading platform
supporting column
jack
oil pressure meter
digital dial gauge
test pile
supporting column
reference beam
digital dial gauge
test pile
loading platform
steel pole

(a) (b)

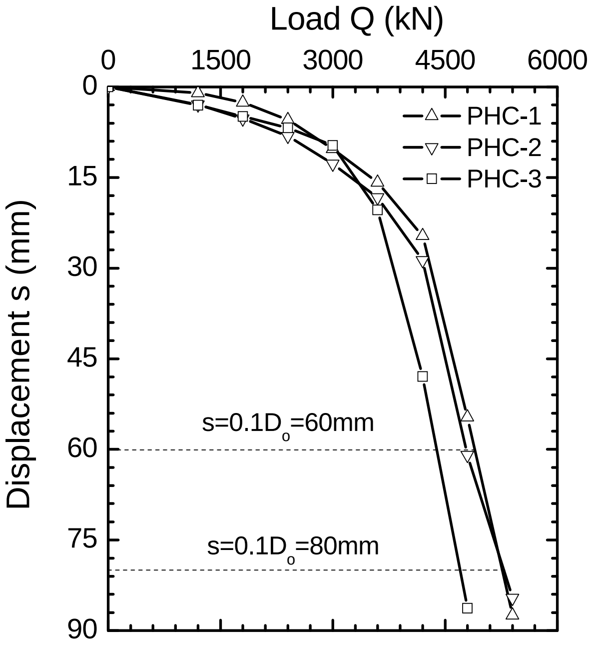

Load Q (kN)
0
1500
3000
4500
6000
Displacement s (mm)
0
15
30
45
60
75
90
PHC-1
PHC-2
PHC-3
s=0.1D$_o$=60mm
s=0.1D$_o$=80mm

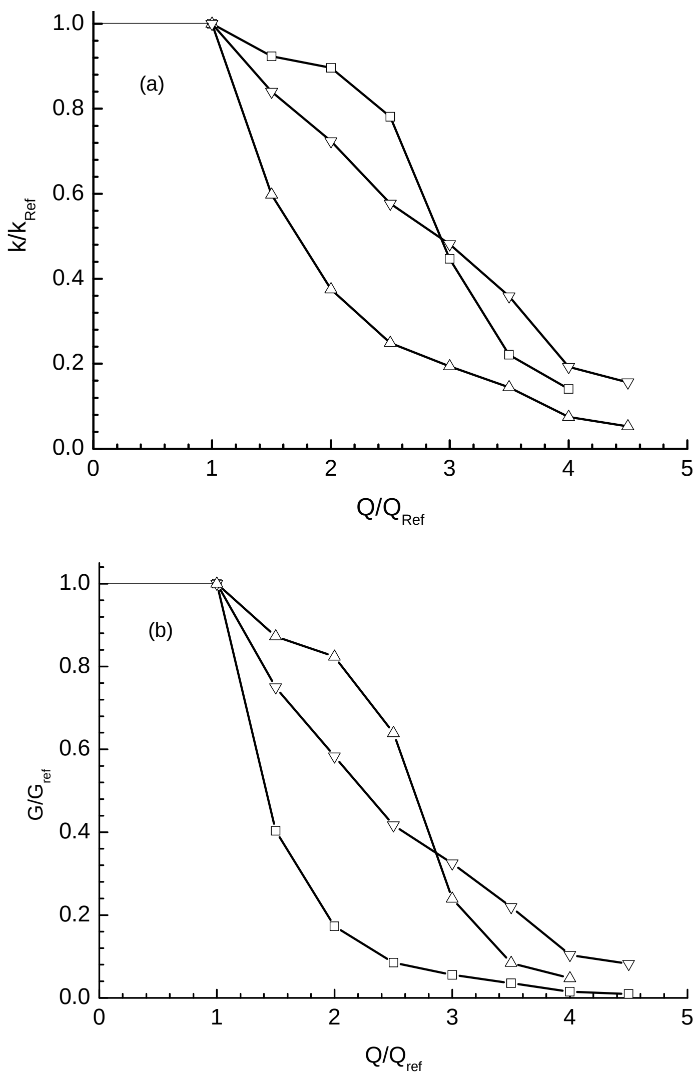

(a)
k/k_Ref
Q/Q_Ref
(b)
G/G_ref
Q/Q_ref
0.0
0.2
0.4
0.6
0.8
1.0
0
1
2
3
4
5

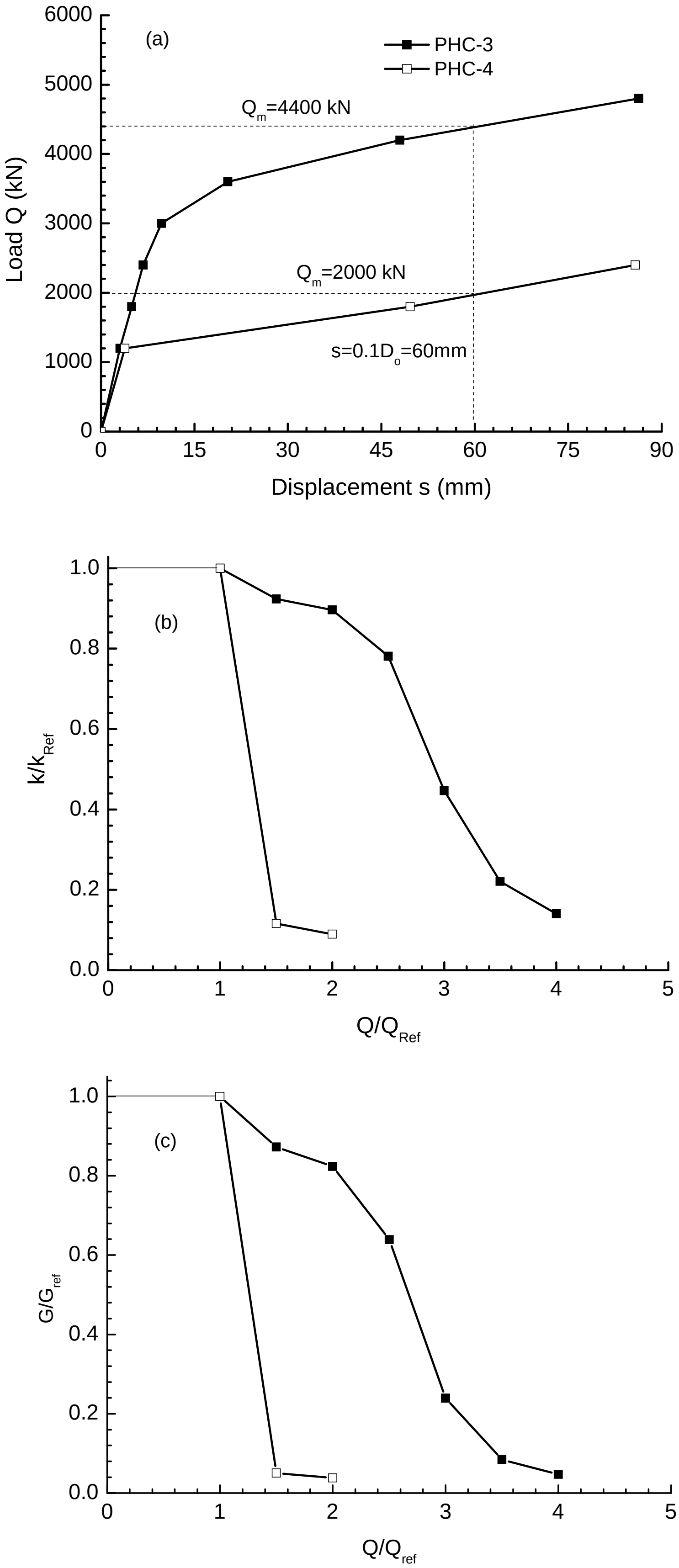

(a)
PHC-3
PHC-4
Q_m=4400 kN
Q_m=2000 kN
s=0.1D_o=60mm
Load Q (kN)
Displacement s (mm)
(b)
k/k_Ref
Q/Q_Ref
(c)
G/G_ref
Q/Q_ref

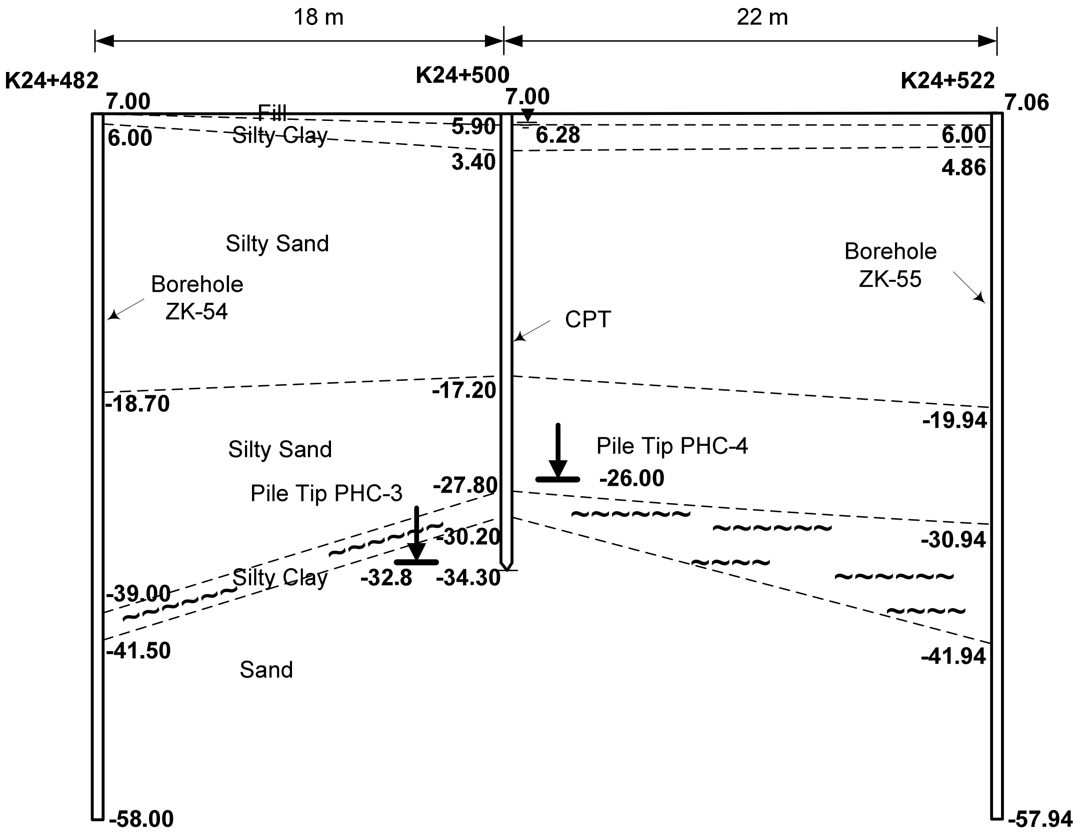
18 m
22 m
K24+482
K24+500
K24+522
7.00
7.00
7.06
Fill
Silty Clay
6.00
5.90
6.28
6.00
3.40
4.86
Silty Sand
Borehole
ZK-54
CPT
Borehole
ZK-55
-18.70
-17.20
-19.94
Silty Sand
Pile Tip PHC-4
-26.00
Pile Tip PHC-3
-27.80
-30.20
-30.94
-32.8
-34.30
Silty Clay
-39.00
-41.50
-41.94
Sand
-58.00
-57.94

Table 1 Summary of pile installations

Pile ID	Date of installation	Location	Diameter D (mm)	Wall thickness (mm)	Embedment (mm)	L/D	Section (m)	Total blows
PHC-1	28/06/2013	K34	600	130	29.3	48.8	12+12+12	816
PHC-2	08/07/2013	K27	800	130	29.2	36.5	12+12+12	1232
PHC-3	29/09/2013	K24+500	600	130	39.8	66.3	13+14+15	1381
PHC-4	13/07/2013	K24+500	600	130	33	55.0	12+12+12	924

Table 2 Summary of the load tests

Pile ID	Age of loaded pile (Days)	Measured total load at s=0.1D (ultimate capacity) Q_m (kN)	Measured total load at s=0.01D (nominal shaft yield points) Q_T (kN)
PHC-1	15	4900	2400
PHC-2	13	5270	2400
PHC-3	14	4400	2050
PHC-4	5	2000	1250

Table 3 Elastic response analysis results. Note: 'Ref' values found under Q=1200kN

Pile ID	$k_{Ref}\times10^{-3}$ (kN/m)	G_{ref} (MPa)	Q_b/Q_T at 0.01D	Interpreted peak shaft Q_s (kN)	Interpreted Q_b at 0.1D (kN)
PHC-1	1176	150	0.02	2352	2548
PHC-2	408	15.7	0.06	2256	3014
PHC-3	396	18.9	0.01	2030	2370
PHC-4	313	31.8	0.03	1213	787

Table 4 Summary of tip q_c and D_r values employed in various calculation methods

Pile ID	Tip q_c (MPa)	Standard $q_{c,avg}$ (MPa) for 3 methods			Tip D_r	Shaft average D_r
		ICP	ICP (lower bound)	UWA/Dutch		
PHC-1	17.98	16.97	–	16.86	0.61	0.47
PHC-2	11.09	10.17	–	10.04	0.48	0.42
PHC-3	11.82	14.33	–	10.84	0.40	0.34
PHC-4	8.24	8.88	3.81	8.27	0.33	0.33

Table 5 Shaft and base calculations (units: kN) and total compression capacity Q_c/Q_m ratios

Pile ID	ICP Calculation Q_c				UWA Calculation Q_c								API Calculation Q_c			
					Full version				Simplified offshore version							
	Shaft	Base	Total	Q_c/Q_m	Shaft	Base	Total	Q_c/Q_m	Shaft	Base	Total	Q_c/Q_m	Shaft	Base	Total	Q_c/Q_m
PHC-1	2243	3257	5500	1.12	2311	2349	4660	0.95	1976	2172	4148	0.85	2363	921	3285	0.67
PHC-2	2271	2782	5053	0.96	2360	2184	4544	0.86	2045	1993	4038	0.77	2525	1081	3607	0.68
PHC-3	2482	2751	5234	1.19	2363	1510	3873	0.88	1929	1396	3325	0.76	3327	1357	4684	1.06

Table 6 Comparisons of shaft capacity predictions for PHC-4 (units: kN)

Interpreted Q_s at t=5 days	Q_s corrected for early age	ICP Q_s	UWA Q_s	API Q_s
1200	1380	1916	1873	2654

Table 7 End bearing predictions of PHC-4 based on various methods (units: kN)

interpreted Q_b	ICP Q_b	ICP * Q_b	UWA Q_b	API Q_b	Xu method ** Q_b	HKU Q_b
800	1958	689	1150	921	1429	836

*: using lowest q_c to estimate the base capacity to account for the underlying soft layer effect

**: applying the reduction factor to ICP 'default' method from Xu (2006)